Check for updates

ADVANCING EARTH AND SPACE SCIENCES

Geophysical Research Letters

RESEARCH LETTER
10.1029/2023GL106784

Leah D. Grant and Bastian Kirsch contributed equally to this work.

Key Points:

- Cold pool impacts on sub-mesoscale temperature variability are quantified using variograms derived from observations and simulations
- Cold pools enhance temperature variability on scales between 5 and 15 km, but the magnitude varies strongly with lifetime and environment
- High-resolution case-study and idealized simulations underestimate the magnitude of cold pool variability, irrespective of resolution

Supporting Information:

Supporting Information may be found in the online version of this article.

Correspondence to:

L. D. Grant and B. Kirsch,
leah.grant@colostate.edu;
bastian.kirsch@uni-hamburg.de;
bastian.kirsch@kit.edu

Citation:

Grant, L. D., Kirsch, B., Bukowski, J., Falk, N. M., Neumaier, C. A., Sakradzija, M., et al. (2024). How variable are cold pools? *Geophysical Research Letters*, *51*, e2023GL106784. https://doi.org/10.1029/2023GL106784

Received 12 OCT 2023
Accepted 1 MAR 2024

Author Contributions:

Conceptualization: Leah D. Grant, Bastian Kirsch
Data curation: Leah D. Grant, Bastian Kirsch, Jennie Bukowski, Nicholas M. Falk, Christine A. Neumaier, Mirjana Sakradzija
Formal analysis: Leah D. Grant, Bastian Kirsch, Jennie Bukowski, Nicholas M. Falk, Christine A. Neumaier
Funding acquisition: Leah D. Grant, Susan C. van den Heever, Felix Ament
Investigation: Leah D. Grant, Bastian Kirsch, Jennie Bukowski,

© 2024. The Authors.
This is an open access article under the terms of the Creative Commons Attribution License, which permits use, distribution and reproduction in any medium, provided the original work is properly cited.

How Variable Are Cold Pools?

Leah D. Grant[1], Bastian Kirsch[2,3,4], Jennie Bukowski[1], Nicholas M. Falk[1], Christine A. Neumaier[1], Mirjana Sakradzija[3,5,6], Susan C. van den Heever[1], and Felix Ament[2,3]

[1]Department of Atmospheric Science, Colorado State University, Fort Collins, CO, USA, [2]Meteorological Institute, University of Hamburg, Hamburg, Germany, [3]Hans Ertel Centre for Weather Research, Offenbach, Germany, [4]Now at Institute of Meteorology and Climate Research Troposphere Research (IMKTRO), Karlsruhe Institute of Technology (KIT), Karlsruhe, Germany, [5]Deutscher Wetterdienst, Offenbach, Germany, [6]Now at Department of Geography, Ludwig-Maximilians-Universität, Munich, Germany

Abstract Cold pools formed by precipitating convective clouds are an important source of mesoscale temperature variability. However, their sub-mesoscale (100 m–10 km) structure has not been quantified, impeding validation of numerical models and understanding of their atmospheric and societal impacts. We assess temperature variability in observed and simulated cold pools using variograms calculated from dense network observations collected during a field experiment and in high-resolution case-study and idealized simulations. The temperature variance in cold pools is enhanced for spatial scales between ∼5 and 15 km compared to pre-cold pool conditions, but the magnitude varies strongly with cold pool evolution and environment. Simulations capture the overall cold pool variogram shape well but underestimate the magnitude of the variability, irrespective of model resolution. Temperature variograms outside of cold pool periods are represented by the range of simulations evaluated here, suggesting that models misrepresent cold pool formation and/or dissipation processes.

Plain Language Summary Cold pools are cool gusty winds beneath thunderstorms that are formed by cooling from rainfall. They have many important impacts in the atmosphere and on society but are difficult to properly simulate in numerical weather models. The variability in cold pool temperature is an understudied feature of cold pools but which is important to represent in numerical models. In this study, we examine cold pool temperature variability from a dense network of surface weather station observations collected during a field campaign, and we compare those observations to numerical simulations of cold pools in a range of environments. We find that cold pools enhance temperature variability for distances greater than ∼5 km but suppress variability on smaller distances, and that the magnitude of cold pool temperature variability is strongly dependent on the environment and cold pool lifetime. We also show that numerical models, even at very high resolutions, are not able to properly simulate the magnitude of cold pool temperature variability. We highlight areas for improvement in numerical models that may help to improve simulations of cold pool variability, including land-atmosphere interactions, turbulence, and conversion processes between water vapor and condensed water in storms.

1. Introduction

Cold pools, regions of dense air formed by precipitation that propagate as density currents (Benjamin, 1968; Byers & Braham, 1949), are ubiquitous atmospheric phenomena that can occur with any type of precipitating cloud. They play a myriad of important roles in weather, climate, and society: they initiate convection and influence convective system properties (e.g., Feng et al., 2015; Khairoutdinov & Randall, 2006; Purdom, 1976; Rotunno et al., 1988; Schlemmer & Hohenegger, 2014; Wilson & Schreiber, 1986), control convective aggregation (Haerter, 2019; Jensen et al., 2022), loft aerosols such as dust and biological particles (Marks et al., 2001; Bou Karam et al., 2014; Seigel & van den Heever, 2012; Bukowski & van den Heever, 2022), and impact aviation operations (Fujita, 1978). In images of laboratory density currents or dust-lofting atmospheric cold pools called haboobs (e.g., see Simpson, 1969, Figure 1, Figure 7), multi-scale turbulent structures are evident, implying that cold pool properties should exhibit variability on scales ranging from meters to the size of the cold pool itself. However, little is known about the magnitude or structure of this variability from observations and numerical simulations. Understanding this variability is crucial to assessing cold pool representation in large-eddy simulation (LES), numerical weather prediction, and climate models, and to comprehending their many atmospheric and societal impacts.

Nicholas M. Falk, Christine A. Neumaier, Mirjana Sakradzija
Methodology: Leah D. Grant, Bastian Kirsch
Project administration: Leah D. Grant, Susan C. van den Heever, Felix Ament
Supervision: Leah D. Grant, Susan C. van den Heever, Felix Ament
Writing – original draft: Leah D. Grant, Bastian Kirsch, Jennie Bukowski, Nicholas M. Falk, Christine A. Neumaier
Writing – review & editing: Leah D. Grant, Bastian Kirsch, Jennie Bukowski, Nicholas M. Falk, Christine A. Neumaier, Mirjana Sakradzija, Susan C. van den Heever, Felix Ament

Previous modeling studies show that simulated cold pool properties, and their interactions with components of the earth system, are sensitive to the model grid spacing (Straka et al., 1993; Bryan et al., 2003; Grant & van den Heever, 2016; Huang et al., 2018; Hirt et al., 2020; Meyer & Haerter, 2020; Fiévet et al., 2023). Many of these studies demonstrated more intense, longer-lived, and faster-propagating cold pools at finer model resolutions. Droegemeier and Wilhelmson (1987) and Straka et al. (1993) showed that turbulent structures in cold pools are not appropriately represented until 100 m or finer grid spacings. Grant and van den Heever (2016) recommended horizontal (vertical) grid spacings of 100 m (50 m) or finer to simulate the impacts of turbulent structures on the cold pool properties, and accurately capture cold pool interactions with the land surface. Hirt et al. (2020) showed that coarser resolutions lead to weaker upward mass flux at cold pool edges, with impacts on convective initiation.

Fewer studies have investigated the observed variability in individual cold pools due to limited spatial resolutions of traditional observing networks. While single-point observations (e.g., Kirsch et al., 2021; Kruse et al., 2022) require assumptions about the atmospheric flow to derive spatial cold pool characteristics, two recent observational campaigns were conducted to directly address this gap. van den Heever et al. (2021) used a *flying curtain* strategy to measure cold pools on scales of 100 m to 1 km in the High Plains of the U.S. They found variations in temperature and wind on scales of 1 km and finer. Dense networks of surface meteorological stations in Germany observed temperature gradients inside a cold pool of up to 9 K/7 km (Hohenegger et al., 2023; Kirsch, Hohenegger, Klocke, Senke, et al., 2022).

As evidenced by this previous work, scale interactions in cold pools are critical to their properties, lifetimes, interactions with earth's surface and convection, and societal impacts. Yet, comprehensive analyses of the scales of temperature variability in observed cold pools have not been performed, nor have these scales been assessed in numerical models. This study aims to fill this important knowledge gap by addressing the following questions, with a focus on cold pool *temperature* as a critical component of cold pool density and hence its first-order properties.

1. What are the scales of temperature variability in observed cold pools?
2. How accurately do numerical models, with grid spacings of order 100 m to 1 km, represent this observed variability?
3. What is the sensitivity of cold pool temperature variability to environmental conditions?

We investigate these questions using novel observations from a recent field campaign, the Field Experiment on Submesoscale Spatio-Temporal Variability in Lindenberg (FESSTVaL; Hohenegger et al., 2023), designed to measure fine spatio-temporal variability in cold pool properties. We assess the ability of numerical models to accurately represent this variability as a function of model resolution and environment, using case-study simulations of observed cold pool events during FESSTVaL, and case-study and idealized simulations of cold pools in a range of other environments. We find that models generally do *not* accurately represent observed variability in cold pool temperatures, even at LES grid spacings, and highlight key areas for improvement in simulating processes contributing to cold pool properties and lifetimes.

2. Methods

2.1. FESSTVaL Observations

The observational data set used in this study was collected during the FESSTVaL field experiment held in eastern Germany from 17 May to 27 August 2021 (Hohenegger et al., 2023). During FESSTVaL, 42 cold pool events were observed (Kirsch, Hohenegger, et al., 2024). The air temperature data were recorded by 99 custom-built, low-cost measurement stations (Kirsch, Hohenegger, Klocke, Senke, et al., 2022), arranged as a dense network covering a 30 km-diameter circular area centered at the Lindenberg observatory. Nearest-neighbor distances ranged from 100 m to 4.8 km (Figure 1a; Figure S1 in Supporting Information S1; Kirsch, Hohenegger, et al., 2024). The network design allows for examination of variability in individual cold pools on scales from 100 m to 15 km. All raw sub-minute temperature data are smoothed with a 1-min running average filter. On 29 June 2021, a cold pool named "Jogi" was observed by the network (Figure 1a; Hohenegger et al., 2023; Kirsch, Hohenegger, et al., 2024). Jogi was among the strongest cold pool events of the campaign, initiating at around 1530 local time (LT) and lasting for ∼2 hr (Figure S2 in Supporting Information S1). Since Jogi's spatial extent and life cycle was largely sampled by the network, it is analyzed in detail in this study.

19448007, 2024, 6, Downloaded from https://agupubs.onlinelibrary.wiley.com/doi/10.1029/2023GL106784, Wiley Online Library on [19/03/2024]. See the Terms and Conditions (https://onlinelibrary.wiley.com/terms-and-conditions) on Wiley Online Library for rules of use; OA articles are governed by the applicable Creative Commons License

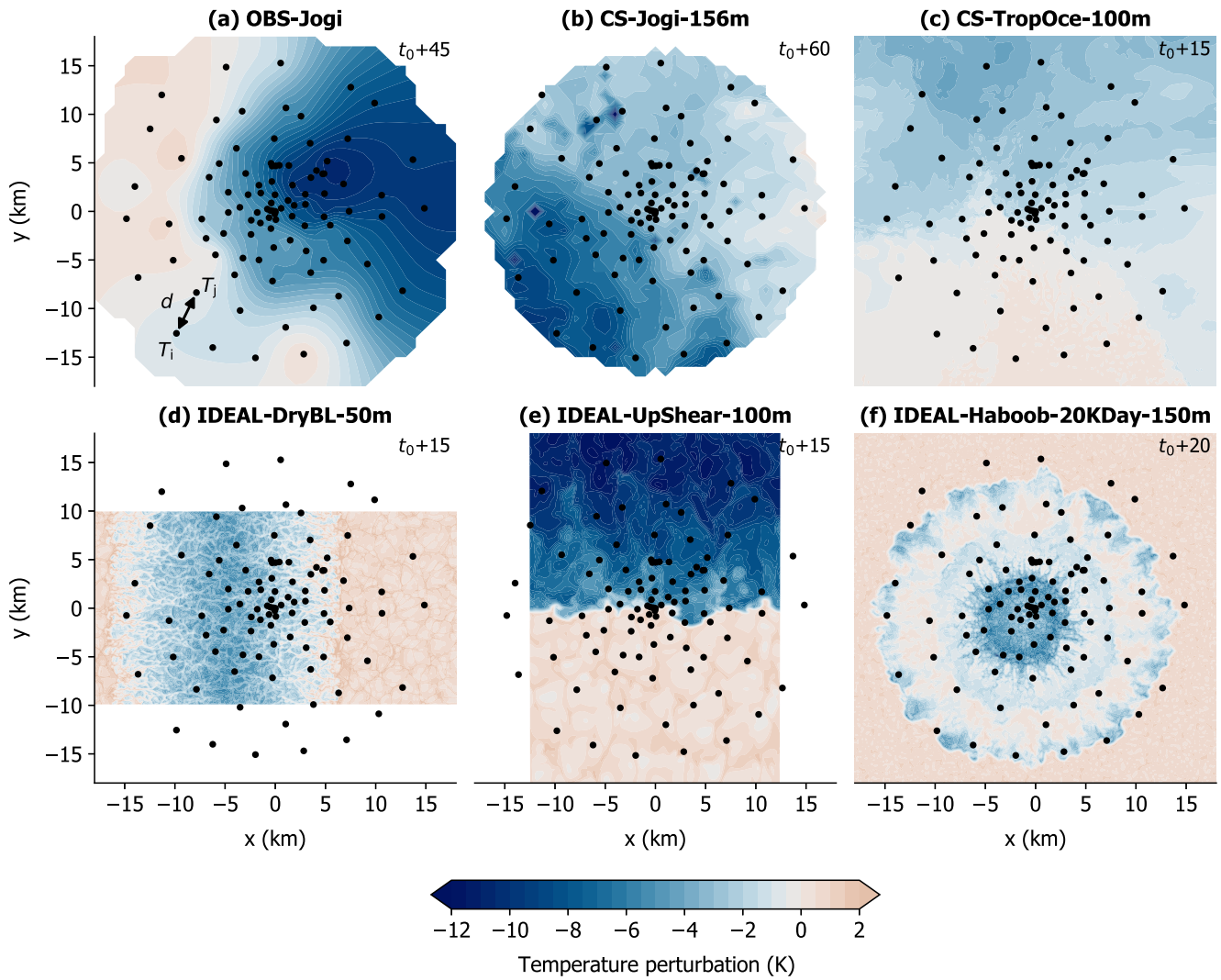

Figure 1. Plan views of temperature perturbations relative to the reference temperature (Table 1) for (a) observations from the Jogi case (spatially interpolated for better visualization), (b) a Jogi case study simulation, and (c)–(f) other case study and idealized simulations. Model data are shown at the lowest level above ground. The time (min) since cold pool onset (t_0), that is, last timestep of unperturbed conditions, is labeled at the top right and the FESSTVaL network is overlain in black dots. Coordinates are relative to the network center. Notations in (a) refer to quantities shown in Equation 1.

2.2. Quantifying Spatial Variability

We quantify the spatial variability of near-surface air temperature using variograms (Chils & Delfiner, 1999; Wackernagel, 2003). Variogram analysis is used in geostatistics to characterize the spatial heterogeneity of a regionalized, stochastic variable. The underlying variogram function of a variable (here: temperature T) sampled at selected locations can be estimated from its empirical variogram ($\hat{\gamma}$). $\hat{\gamma}$ is calculated by forming pairs of sample locations $i \neq j$ and binning them according to their distances d (Figure 1a). The variogram function for distance bin d, with $N(d)$ samples, is given by:

$$\hat{\gamma}(d) = \frac{1}{2}\frac{1}{N(d)}\sum_{i \neq j}\left(T_j - T_i\right)^2 \tag{1}$$

Thus, the variogram function quantifies the degree of spatial variance across different length scales within a sampled temperature field. The information content of the variogram depends on the spatial distribution of sampling locations and the distance bins used. As a trade-off between distance resolution and statistical robustness, especially for distances smaller than ~3 km, we choose a 500 m bin width to calculate all empirical

19448007, 2024, 6, Downloaded from https://agupubs.onlinelibrary.wiley.com/doi/10.1029/2023GL106784, Wiley Online Library on [19/03/2024]. See the Terms and Conditions (https://onlinelibrary.wiley.com/terms-and-conditions) on Wiley Online Library for rules of use; OA articles are governed by the applicable Creative Commons License

Table 1
Names and Cold Pool Properties for OBS-Jogi and Selected Simulations

Name	T_{ref} (°C)[a]	ΔT_{mean}, ΔT_{min} (K)[b]	σ_{mean}, σ_{max} (K)[b]
OBS-Jogi	28.6	−2.7, −11.5	2.51, 3.40
CS-Jogi-156m	29.0	−0.8, −9.5	1.07, 2.04
CS-TropOce-100m	27.3	−1.6, −4.4	0.69, 1.05
IDEAL-DryBL-50m	28.5	−1.0, −9.7	1.27, 3.28
IDEAL-DownShear-100m	20.9	−6.6, −15.6	1.61, 4.62
IDEAL-UpShear-100m	20.9	−3.7, −16.8	3.05, 4.95
IDEAL-Haboob-20KDay-150m	43.28	−1.15, −15.77	1.62, 6.24

Note. Simulations are named beginning with IDEAL (idealized) or CS (case study), followed by a description of the environment and the horizontal grid spacing. [a]T_{ref}: Mean temperature across all stations and over 1-hr period before cold pool onset. [b]ΔT_{mean}, ΔT_{min}, σ_{mean}, σ_{max}: Mean temperature (T) or standard deviation (σ) across all stations and over 1-hr period after cold pool onset, or minimum/maximum across all stations and cold pool lifetime.

variograms (Figure S1 in Supporting Information S1). The maximum variogram distance corresponds to half the domain size (15 km; Wackernagel, 2003). Variograms are calculated for observed FESSTVaL data and in the simulation data by superimposing the station network on the model grid and linearly interpolating the model data at the lowest level above ground to the station locations. The calculation utilizes all available station data at a given time step.

2.3. Simulations

A collection of simulation sets is analyzed to examine simulated cold pool variability in a range of environments and model resolutions. These include case study simulations of cold pool Jogi and a tropical maritime cold pool, and three sets of idealized cold pool simulations in dry continental conditions with varying background environments. All simulation names, grid spacings, output frequencies, FESSTVaL network placements, and cold pool lifetimes are summarized in Table S1 in Supporting Information S1, while cold pool properties for one simulation in each set are in Table 1.

2.3.1. CS-Jogi Simulations

Case-study simulations for cold pool Jogi uses the Icosahedral Nonhydrostatic model in LES mode (ICON-LES; Dipankar et al., 2015; Text S1 in Supporting Information S1). The setup consists of four elliptical domains with grid spacings of 625 m, 312 m, 156 m (see Figure 1b), and 75 m, centered around the FESSTVaL experiment area in eastern Germany. The maximum diameter of the CS-Jogi-75m simulation domain is 24 km and smaller than the FESSTVaL network. Thus, variograms are shown only to 10 km (Figure S1 in Supporting Information S1).

2.3.2. CS-TropOce Simulations

Case-study simulations with 1 km horizontal grid spacing are performed using the Regional Atmospheric Modeling System (RAMS; Cotton et al., 2003; Saleeby & van den Heever, 2013) for the NASA Cloud, Aerosol, and Monsoon Processes Philippines Experiment (CAMP^{2}Ex; Reid et al., 2023, S.3.2). Includes a coarse and high-resolution simulation of a cold pool that occurred west of Luzon (simulation CS-TropOce-1km; Text S1 in Supporting Information S1; and CS-TropOce-100m; Text S1 in Supporting Information S1; Figure 1c).

2.3.3. IDEAL-DryBL Simulations

A RAMS idealized LES of a linear cold pool dissipating by surface fluxes and entrainment in a deep, turbulent boundary layer (IDEAL-DryBL-50m, Figure 1d; Grant & van den Heever, 2018). Initial land surface and atmospheric conditions are horizontally homogeneous, and there is no background wind shear, interactions with clouds, nor microphysical processes. A coarser simulation (IDEAL-DryBL-100m) is also included.

19448007, 2024, 6, Downloaded from https://agupubs.onlinelibrary.wiley.com/doi/10.1029/2023GL106784, Wiley Online Library on [19/03/2024]. See the Terms and Conditions (https://onlinelibrary.wiley.com/terms-and-conditions) on Wiley Online Library for rules of use; OA articles are governed by the applicable Creative Commons License

2.3.4. IDEAL-Shear Simulations

RAMS simulations similar to IDEAL-DryBL, except the environment includes ∼20 m s^{-1} vertical wind shear over the lowest 3 km, and the *x*-direction is a narrow channel (Text S1 in Supporting Information S1). Two horizontal grid spacings are included (IDEAL-Shear-100m (Figure 1e) and IDEAL-Shear-250m). In both simulations, two networks are imposed: one downshear and one upshear, called the IDEAL-DownShear and IDEAL-UpShear (Figure 1e). The background wind speed limits the upshear cold pool propagation while increasing the downshear leading edge propagation speed.

2.3.5. IDEAL-Haboob-150m Simulations

Bukowski and van den Heever (2022) describe a 120-simulation ensemble of idealized dust-producing cold pools (haboobs) in an arid, desert-like environment using RAMS, a single circular cold bubble, and no background winds or microphysical processes. Eight simulations are subset from the ensemble: four each during daytime and nighttime with initial cold pool temperature deficits ranging from 10 to 20 K (Figure 1f; see Section 3.3).

3. Results

3.1. Observed Temperature Variability

To address our first science question, we examine the variogram for the 42 cold pools observed throughout the 103-day FESSTVaL campaign (Figure 2a). As a baseline, we also analyze the variogram for all daytime non-cold pool periods. On average, cold pools enhance temperature variance on spatial scales between 5 and 15 km. As previous studies show, cold pools tend to be at least 5 km in diameter (Feng et al., 2015; Kirsch, Hohenegger, Klocke, Senke, et al., 2022, 2024; Terai & Wood, 2013) and introduce footprints in the temperature field on the scale of the cold pool itself. Footprints are larger in spatial scale than temperature variations caused by boundary layer processes such as Rayleigh-Benard convection (Lord Rayleigh, 1916), which tend to scale with the boundary layer depth (e.g., Hardy & Ottersten, 1969). Interestingly, Figure 2a also indicates that on average, cold pools reduce temperature variance on spatial scales less than ∼4 km. This may indicate mechanical mixing by the enhanced winds within relative to outside the cold pool. Additionally, cold pools are stably stratified (Kirsch et al., 2021; Kruse et al., 2022) and may suppress surface sensible heat fluxes, reducing surface-driven turbulence; although, previous studies suggest sensible heat fluxes can be enhanced within cold pools under certain conditions (Grant & van den Heever, 2016, 2018a; Gentine et al., 2016; Bukowski & van den Heever, 2021). Finally, note the different shapes of the cold pool and non-cold pool variograms: the daytime non-cold pool variogram slope is steeper at small scales but flattens out at scales above ∼5 km, indicating that the dominant scales of variability due to boundary layer motions are 5 km and smaller. However, the cold pool variogram slope is more linear across the range of scales.

We next examine the variogram results for the Jogi case (OBS-Jogi; Figure 2b). While most cold pools from the FESSTVaL record (31) had median temperature deficits of 4 K or weaker (Kirsch, Hohenegger, et al., 2024), the Jogi cold pool had a maximum temperature deficit of 11.5 K (Table 1). This is in line with previous observations of strong cold pools (e.g., Engerer et al., 2008; Kirsch et al., 2021; van den Heever et al., 2021). The OBS-Jogi temperature variogram is almost an order of magnitude larger than the average variograms for other observed cold pools (Figure 2b). This indicates that the strongest cold pools can have exceptionally high magnitude variograms compared to cold pools overall, and that the relative enhancement in temperature variance for strong cold pools is greater than the relative enhancement in mean cold pool strength.

3.2. Comparing Observed and Simulated Temperature Variability

We address our second question by comparing the CS-Jogi case-study simulations to the observations (Figure 2b). While the temperature variogram in the simulated Jogi cold pools have the correct shape, they are too weak, with median magnitudes ∼1/3 of the observations and outside the OBS-Jogi interquartile range. This finding is irrespective of whether the variance is examined across the entire network or only within the cold pools (Figure S3 in Supporting Information S1). Remarkably, the model resolution does not systematically impact the simulated temperature variance beyond the statistical noise level. Nevertheless, all four CS-Jogi simulations well approximate the mean cold pool temperature deficit and its temporal evolution (Figures 1a and 1b; Figure S2 in Supporting Information S1). In fact, the simulations have an even stronger mean temperature deficit than the

19448007, 2024, 6, Downloaded from https://agupubs.onlinelibrary.wiley.com/doi/10.1029/2023GL106784, Wiley Online Library on [19/03/2024]. See the Terms and Conditions (https://onlinelibrary.wiley.com/terms-and-conditions) on Wiley Online Library for rules of use; OA articles are governed by the applicable Creative Commons License

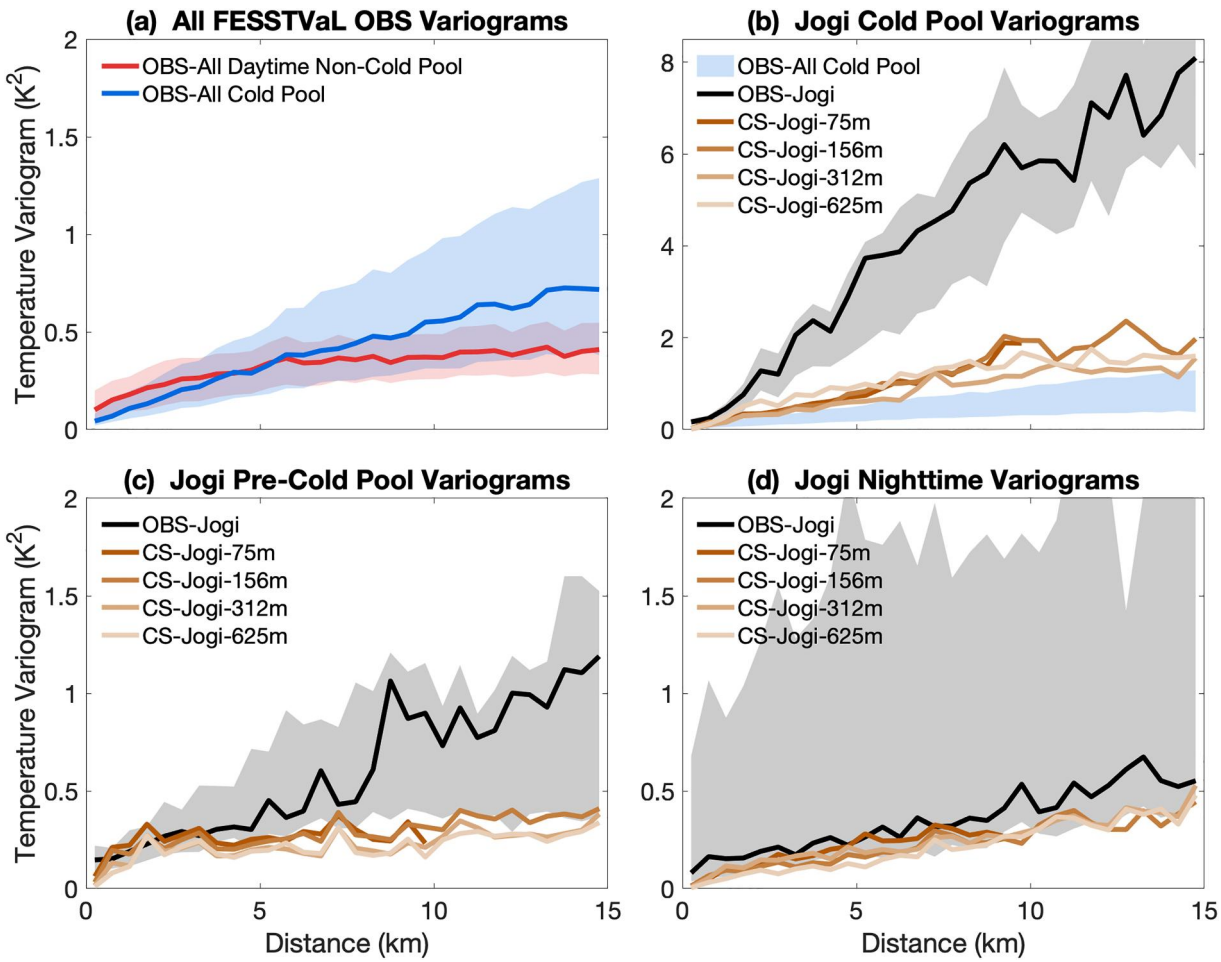

Figure 2. (a) Temperature variograms during cold pool (2 hr after onset) and daytime (1100–1800 LT) non-cold time periods every 15 min for the entire duration of the FESSTVaL data set. (b) Comparison between all observed cold pools (blue shading, same as in panel (a)), the OBS-Jogi case every 1 min, and the CS-Jogi simulations. Note the different *y*-axis scale compared to the other panels. (c) Variograms for 3-hr periods before cold pool onset for Jogi observations and simulations. (d) As in (c) but over nighttime periods (2200–0500 LT). All solid lines (shading) represent the median (interquartile range).

observations (Figure S2 in Supporting Information S1), although the maximum deficit at any one station and the standard deviations across the network are larger in the observations (Table 1). Overall, this demonstrates that temperature variance is not properly represented even when the mean cold pool properties are well-simulated.

To assess reasons for the simulation's misrepresentation of the observed cold pool temperature variance, we examine variograms in the pre-cold pool (Figure 2c) and nocturnal boundary layer (Figure 2d). Pre-cold pool variograms are well-simulated at small scales, but underestimated at scales above ~5 km (Figure 2c). The larger-scale variance underestimation stems from a small pre-Jogi cold pool in the observations which enhances the variogram magnitude above 8 km but isn't present in the simulations (not shown). The agreement below 5 km indicates that the scales of variability induced by boundary layer circulations are well-represented in the simulations. Second, the nighttime variogram magnitudes in the CS-Jogi simulations are slightly underestimated but within the OBS-Jogi interquartile range (Figure 2d). At night when the boundary layer stabilizes, temperature variance is primarily driven by topographic-driven differences in station elevations across the FESSTVaL network. The agreement between the nighttime CS-Jogi and OBS-Jogi data indicates the topography is also well-resolved in the simulations, consistent with the fine spatial resolution of the ICON-LES input topography data (Text S1 in Supporting Information S1). Overall, the non-cold pool variogram comparisons suggest that the model underestimation of cold pool temperature variability is *not* due to misrepresentation of boundary layer circulations, surface heterogeneity, or topography. Rather, it's likely from poor representation of processes contributing to internal cold pool variability, like spatial variations in evaporative cooling rates, turbulence mixing, and responding surface fluxes within the cold pool.

19448007, 2024, 6, Downloaded from https://agupubs.onlinelibrary.wiley.com/doi/10.1029/2023GL106784, Wiley Online Library on [19/03/2024]. See the Terms and Conditions (https://onlinelibrary.wiley.com/terms-and-conditions) on Wiley Online Library for rules of use; OA articles are governed by the applicable Creative Commons License

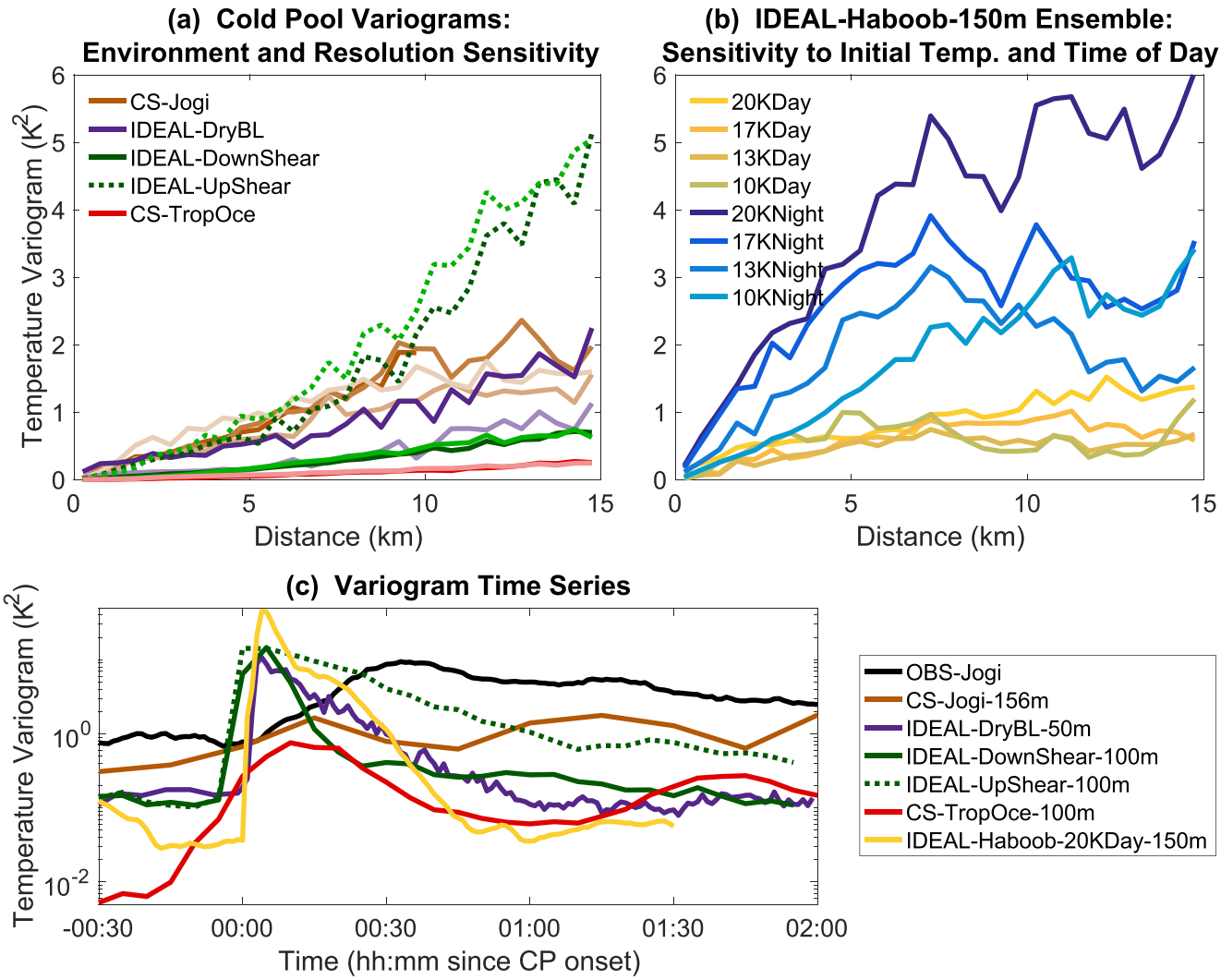

Figure 3. (a) As in Figure 2b, but comparing the impact of environment and model grid spacing on median variogram magnitudes. Darker colors indicate higher resolution simulations. (b) Median variograms for the IDEAL-Haboob-150m ensemble, showing variation in variogram magnitudes as a function of initial cold pool temperature and day (yellow lines) versus night (blue lines). (c) Time series of median variogram magnitude across all bins for OBS-Jogi and select simulations. Note the log *y*-axis scaling.

3.3. Sensitivity of Cold Pool Variability to Environment and Model Resolution

Here, we further answer our second science question and address our third question. Figures 3a and 3b summarize the strong control of the environment on cold pool temperature variance. Cold pools forming in contrasting environments, such as tropical maritime versus midlatitude continental, can have over an order of magnitude difference in temperature variograms (compare CS-TropOce-100m to IDEAL-UpShear-100m; Figures 3a, 1c and 1e). Tropical maritime cold pools are typically much weaker than midlatitude continental ones (Table 1, Figure 1, Zuidema et al., 2012; van den Heever et al., 2021; Simoes-Sousa et al., 2022) and to first order, one might expect weaker cold pools to exhibit smaller variability. The IDEAL-Haboob ensemble, in which the initial cold pool temperature deficit was varied, confirms this point (Figure 3b): initially stronger cold pools have larger temperature variance. Second, cold pool temperature variance can be vastly different even in the same background environment, as evidenced by the variogram differences between the upshear and downshear sides of the cold pool in the IDEAL-Shear simulations arising from different residence times in the network (Figure 3a). Third, the IDEAL-Haboob ensemble (Figure 3b) shows that all else equal, nocturnal cold pools have larger temperature variability than during the day, and nighttime cold pool variability is more sensitive to the cold pool strength than during the daytime. Daytime cold pools dissipate faster than the nighttime ones due to surface sensible heating

19448007, 2024, 6, Downloaded from https://agupubs.onlinelibrary.wiley.com/doi/10.1029/2023GL106784, Wiley Online Library on [19/03/2024]. See the Terms and Conditions (https://onlinelibrary.wiley.com/terms-and-conditions) on Wiley Online Library for rules of use; OA articles are governed by the applicable Creative Commons License

and mixing with the turbulent boundary layer (Bukowski & van den Heever, 2022), thus demonstrating the important control of cold pool dissipation processes on temperature variability.

Figure 3a reconfirms the results from the CS-Jogi simulation set (Figure 2b): remarkably, resolution does not strongly impact simulated cold pool temperature variability, counter to what we might expect based on prior literature showing more intense cold pools with finer resolution (see Section 1). The largest difference in variogram magnitude with increasing resolution is in the IDEAL-DryBL simulation set, which has the highest resolution overall and is the only LES set where the vertical grid spacing is also varied, both of which may enhance the change in variogram magnitude.

In the simulations and observations (Figure 3c), there is large temporal variability in cold pool temperature variance, with the greatest magnitudes near cold pool onset. However, the variogram magnitude drops off quickly toward pre-cold pool values in most simulations, especially in continental cold pools undergoing fast dissipation processes (e.g., IDEAL-DryBL-50m, IDEAL-Shear-100m, and IDEAL-Haboob). This again underscores the importance of processes influencing cold pool lifetimes in contributing to the magnitude and evolution of cold pool variability. Finally, while some simulations exhibit peak variogram magnitudes equal to or exceeding the peak for OBS-Jogi, none come close to the OBS-Jogi median variogram magnitude (compare Figure 2b with Figures 3a and 3b), despite some of the simulated cold pools exhibiting similar or larger temperature deficits than OBS-Jogi (e.g., IDEAL-Shear-100m; Table 1). Thus, even when mean cold pool properties are similar to (or stronger than) observed, simulated cold pool temperature variability is still not properly represented at LES resolutions.

4. Conclusions

We have investigated the footprints of cold pools on temperature variability, their representation in numerical models, and their sensitivity to environmental conditions using novel fine-spatio-temporal resolution measurements from the FESSTVaL field campaign, case-study simulations of a FESSTVaL cold pool event, and a collection of case-study and idealized simulations. This is an essential research topic not investigated previously but crucial for understanding cold pool processes, their interactions with convection and earth's surface, and their societal impacts. Variograms are an effective tool to characterize temperature variability and can be applied to model simulations and dense station network observations, enabling easy and fair comparisons. We investigated the following three science questions.

1. *What are the scales of temperature variability in observed cold pools?* The FESSTVaL observations show cold pools enhance spatial temperature variability on scales greater than ~5 km, but suppress variability on smaller scales, likely by mechanical mixing of boundary layer circulations. The magnitude of cold pool temperature variability is highly temporally variable and greatly enhanced for stronger cold pools.
2. *How accurately do numerical models, with grid spacings of order 100 m to 1 km, represent this observed variability?* By comparing an observed cold pool with case study simulations of the same event, we find that numerical models substantially underestimate the observed cold pool temperature variability, even when the mean cold pool properties are well represented. Finer resolution does not significantly improve model representation of cold pool variability.
3. *What is the sensitivity of cold pool temperature variability to environmental conditions?* The suite of simulations examined here demonstrates strong sensitivity of the variability to environmental conditions. Tropical maritime cold pools are less variable than midlatitude continental ones. Cold pool variability is also sensitive to background wind shear, time of day, and cold pool strength, with stronger cold pools exhibiting larger variability.

Through the analysis of pre-cold pool and nighttime temperature variance in non-cold pool conditions, along with the evolution of cold pool temperature variability, we conclude that models likely underestimate the magnitude of cold pool temperature variability due to misrepresentation of physical processes contributing to cold pool lifetimes, namely, latent cooling stemming from microphysical processes and dissipation by entrainment and surface fluxes. The artificial smoothing of temperature gradients and underestimation of internal cold pool variability in simulations can impact vertical velocities and vortical mixing, which affect the representation of convective processes such as convective initiation, storm organization, longevity, and dissipation, as well as preconditions for subsequent convection. These are critical areas for future investigation on process-based understanding and development of numerical models if we are to improve predictions of cold pools and their implications for weather, climate, and society.

19448007, 2024, 6, Downloaded from https://agupubs.onlinelibrary.wiley.com/doi/10.1029/2023GL106784, Wiley Online Library on [19/03/2024]. See the Terms and Conditions (https://onlinelibrary.wiley.com/terms-and-conditions) on Wiley Online Library for rules of use; OA articles are governed by the applicable Creative Commons License

Data Availability Statement

All scripts and NetCDF files containing variogram and model output data used to create figures and tables in this manuscript and supporting information are available on GitHub (Kirsch, Grant, et al., 2024). The APOLLO and WXT observational data sets of FESSTVaL 2021 are available from Universität Hamburg (Kirsch, Hohenegger, Klocke, & Ament, 2022). Model output and/or source code for each set of simulations used in the analyses is available from the following sources.

- CS-Jogi simulations: Sakradzija (2023). See also the FESSTVaL final report at https://fesstval.de/fileadmin/user_upload/fesstval/Files/FESSTVaL-Report-final.pdf (accessed 2023-10-09)
- CS-TropOce simulations: Falk et al. (2023).
- IDEAL-DryBL simulations: Grant and van den Heever (2018b).
- IDEAL-Shear simulations: Neumaier et al. (2023).
- IDEAL-Haboob-150m ensemble: Bukowski and van den Heever (2023).

Acknowledgments
Funding was provided by the Hans Ertel Centre for Weather Research (HErZ) of the German Weather Service (DWD) and the German Federal Ministry of Transport and Digital Infrastructure Grant 4818DWDP1B and the German Research Foundation DFG under Germany's Excellence Strategy, EXC 2037 CLICCS, Project 390683824, the National Science Foundation Grants AGS-2029611, AGS-2105938, and AGS-2019947, and the National Aeronautics and Space Administration Grant 80NSSC18K0149. We acknowledge financial support from the Open Access Publication Fund of Universität Hamburg, high-performance computing support from Cheyenne (doi:10.5065/D6RX99HX) provided by NCAR's Computational and Information Systems Laboratory, sponsored by the National Science Foundation, and the NASA High-End Computing (HEC) Program through the NASA Advanced Supercomputing (NAS) Division at Ames Research Center. LDG and BK have contributed equally to this work. We thank two anonymous reviewers whose comments improved the manuscript clarity and content. Open Access funding enabled and organized by Projekt DEAL.

References

Benjamin, T. B. (1968). Gravity currents and related phenomena. *Journal of Fluid Mechanics*, *31*(02), 209–248. https://doi.org/10.1017/S0022112068000133

Bou Karam, D., Williams, E., Janiga, M., Flamant, C., McGraw-Herdeg, M., Cuesta, J., et al. (2014). Synoptic-scale dust emissions over the Sahara Desert initiated by a moist convective cold pool in early August 2006. *Quart. J. Roy. Meteor. Soc.*, *140*(685), 2591–2607. https://doi.org/10.1002/qj.2326

Bryan, G. H., Wyngaard, J. C., & Fritsch, J. M. (2003). Resolution requirements for the simulation of deep moist convection. *Monthly Weather Review*, *131*(10), 2394–2416. https://doi.org/10.1175/1520-0493(2003)131<2394:rrftso>2.0.co;2

Bukowski, J., & van den Heever, S. (2023). Data from: The impact of land surface properties on haboobs and dust lofting [Dataset]. *Dryad*. https://doi.org/10.5061/dryad.6hdr7sr4d

Bukowski, J., & van den Heever, S. C. (2021). Direct radiative effects in haboobs. *Journal of Geophysical Research: Atmospheres*, *126*(21), e2021JD034814. https://doi.org/10.1029/2021JD034814

Bukowski, J., & van den Heever, S. C. (2022). The impact of land surface properties on haboobs and dust lofting. *Journal of the Atmospheric Sciences*, *79*(12), 3195–3218. https://doi.org/10.1175/JAS-D-22-0001.1

Byers, H. R., & Braham, R. R., Jr. (1949). *The thunderstorm* (p. 287). U.S. Govt. Printing Office.

Chils, J., & Delfiner, P. (1999). *Geostatistics: Modeling spatial uncertainty*. John Wiley Sons, Inc. https://doi.org/10.1002/9780470316993

Cotton, W. R., Pielke, R. A., Walko, R. L., Liston, G. E., Tremback, C. J., Jiang, H., et al. (2003). RAMS 2001: Current status and future directions. *Meteorology and Atmospheric Physics*, *82*(1–4), 5–29. https://doi.org/10.1007/s00703-001-0584-9

Dipankar, A., Stevens, B., Heinze, R., Moseley, C., Zängl, G., Giorgetta, M., & Brdar, S. (2015). Large eddy simulation using the general circulation model ICON. *Journal of Advances in Modeling Earth Systems*, *7*(3), 963–986. https://doi.org/10.1002/2015MS000431

Droegemeier, K., & Wilhelmson, R. (1987). Numerical simulation of thunderstorm outflow dynamics. Part I: Outflow sensitivity experiments and turbulence dynamics. *Journal of the Atmospheric Sciences*, *44*(8), 1180–1210. https://doi.org/10.1175/1520-0469(1987)044<1180:NSOTOD>2.0CO;2

Engerer, N. A., Stensrud, D. J., & Coniglio, M. C. (2008). Surface characteristics of observed cold pools. *Monthly Weather Review*, *136*(12), 4839–4849. https://doi.org/10.1175/2008MWR2528.1

Falk, N. M., Grant, L. D., & van den Heever, S. C. (2023). Code for CS-TropOce simulations (v2.0.0) [Dataset]. *Zenodo*. https://doi.org/10.5281/zenodo.8411499

Feng, Z., Hagos, S., Rowe, A. K., Burleyson, C. D., Martini, M. N., & de Szoeke, S. P. (2015). Mechanisms of convective cloud organization by cold pools over tropical warm ocean during the AMIE/DYNAMO field campaign. *Journal of Advances in Modeling Earth Systems*, *7*(2), 357–381. https://doi.org/10.1002/2014MS000384

Fiévet, R., Meyer, B., & Haerter, J. O. (2023). On the sensitivity of convective cold pools to mesh resolution. *Journal of Advances in Modeling Earth Systems*, *15*(8), e2022MS003382. https://doi.org/10.1029/2022MS003382

Fujita, T. T. (1978). *Manual of downburst identification for project NIMROD* (p. 104). University of Chicago.

Gentine, P., Garelli, A., Park, S.-B., Nie, J., Torri, G., & Kuang, Z. (2016). Role of surface heat fluxes underneath cold pools. *Geophysical Research Letters*, *43*(2), 874–883. https://doi.org/10.1002/2015GL067262

Grant, L. D., & van den Heever, S. C. (2016). Cold pool dissipation. *J.Geophys. Res.-Atmos.*, *121*(3), 1138–1155. https://doi.org/10.1002/2015jd023813

Grant, L. D., & van den Heever, S. C. (2018a). Cold pool-land surface interactions in a dry continental environment. *Journal of Advances in Modeling Earth Systems*, *10*(7), 1513–1526. https://doi.org/10.1029/2018MS001323

Grant, L. D., & van den Heever, S. C. (2018b). RAMS model simulation output for "Cold pool - Land surface interactions in a dry continental environment" [Dataset]. *Mountain Scholar*. https://doi.org/10.25675/10217/186403

Haerter, J. O. (2019). Convective self-aggregation as a cold pool-driven critical phenomenon. *Geophysical Research Letters*, *46*(7), 4017–4028. https://doi.org/10.1029/2018GL081817

Hardy, K. R., & Ottersten, H. (1969). Radar investigations of convective patterns in the clear atmosphere. *Journal of the Atmospheric Sciences*, *26*(4), 666–672. https://doi.org/10.1175/1520-0469(1969)26,666:RIOCPI.2.0.CO;2

Hirt, M., Craig, G. C., Schäfer, S. A. K., Savre, J., & Heinze, R. (2020). Cold pool driven convective initiation: Using causal graph analysis to determine what convection permitting models are missing. *The Quarterly Journal of the Royal Meteorological Society*, *146*(730), 2205–2227. https://doi.org/10.1002/qj.3788

Hohenegger, C., Ament, F., Beyrich, F., Löhnert, U., Rust, H., Bange, J., et al. (2023). FESSTVaL: The Field Experiment on Submesoscale Spatio-Temporal Variability in Lindenberg. *Bulletin of the American Meteorological Society*, *104*(10), E1875–E1892. https://doi.org/10.1175/BAMS-D-21-0330.1

19448007, 2024, 6, Downloaded from https://agupubs.onlinelibrary.wiley.com/doi/10.1029/2023GL106784, Wiley Online Library on [19/03/2024]. See the Terms and Conditions (https://onlinelibrary.wiley.com/terms-and-conditions) on Wiley Online Library for rules of use; OA articles are governed by the applicable Creative Commons License

Huang, Q., Marsham, J. H., Tian, W., Parker, D. J., & Garcia-Carreras, L. (2018). Large-eddy simulation of dust-uplift by a haboob density current. *Atmospheric Environment*, *179*, 31–39. https://doi.org/10.1016/j.atmosenv.2018.01.048

Jensen, G. G., Fiévet, R., & Haerter, J. O. (2022). The diurnal path to persistent convective self-aggregation. *Journal of Advances in Modeling Earth Systems*, *14*(5), e2021MS002923. https://doi.org/10.1029/2021MS002923

Khairoutdinov, M., & Randall, D. (2006). High-resolution simulation of shallow-to-deep convection transition over land. *Journal of the Atmospheric Sciences*, *63*(12), 3421–3436. https://doi.org/10.1175/JAS3810.1

Kirsch, B., Ament, F., & Hohenegger, C. (2021). Convective cold pools in long-term boundary layer mast observations. *Monthly Weather Review*, *149*(3), 811–820. https://doi.org/10.1175/MWR-D-20-0197.1

Kirsch, B., Grant, L. D., Bukowski, J., Falk, N. M., & Neumaier, C. A. (2024). Analysis code and data for Grant and Kirsch et al., "How Variable are Cold Pools?" (GRL, 2024), v1.1 [Dataset]. *Zenodo*. https://doi.org/10.5281/zenodo.10695727

Kirsch, B., Hohenegger, C., & Ament, F. (2024). Morphology and growth of convective cold pools observed by a dense station network in Germany. *The Quarterly Journal of the Royal Meteorological Society*, *150*(759), 857–876. https://doi.org/10.1002/qj.4626

Kirsch, B., Hohenegger, C., Klocke, D., & Ament, F. (2022). Meteorological network observations by APOLLO and WXT weather stations during FESSTVaL 2021 (Version 00-2) [Dataset]. *Integrated Climate Data Center, Universität Hamburg*. https://doi.org/10.25592/uhhfdm.10179

Kirsch, B., Hohenegger, C., Klocke, D., Senke, R., Offermann, M., & Ament, F. (2022). Sub-mesoscale observations of convective cold pools with a dense station network in Hamburg, Germany. *Earth System Science Data*, *14*(8), 3531–3548. https://doi.org/10.5194/ESSD-14-3531-2022

Kruse, I. L., Haerter, J. O., & Meyer, B. (2022). Cold pools over The Netherlands: A statistical study from tower and radar observations. *The Quarterly Journal of the Royal Meteorological Society*, *148*(743), 711–726. https://doi.org/10.1002/qj.4223

Lord Rayleigh, O. M. F. R. S. (1916). LIX. On convection currents in a horizontal layer of fluid, when the higher temperature is on the under side. *The London, Edinburgh and Dublin Philosophical Magazine and Journal of Science*, *32*(192), 529–546. https://doi.org/10.1080/14786441608635602

Marks, G. B., Colquhoun, J. R., Girgis, S. T., Koski, M. H., Treloar, A. B. A., Hansen, P., et al. (2001). Thunderstorm outflows preceding epidemics of asthma during spring and summer. *Thorax*, *56*(6), 468–471. https://doi.org/10.1136/thx.56.6.468

Meyer, B., & Haerter, J. O. (2020). Mechanical forcing of convection by cold pools: Collisions and energy scaling. *Journal of Advances in Modeling Earth Systems*, *12*(11), e2020MS002281. https://doi.org/10.1029/2020MS002281

Neumaier, C. A., Grant, L. D., & van den Heever, S. C. (2023). Code for IDEAL-shear simulations (v1.1.2) [Dataset]. *Zenodo*. https://doi.org/10.5281/zenodo.10402907

Purdom, J. F. W. (1976). Some uses of high-resolution GOES imagery in the mesoscale forecasting of convection and its behavior. *Monthly Weather Review*, *104*(12), 1474–1483. https://doi.org/10.1175/1520-0493(1976)104<1474:SUOHRG>2.0.CO;2

Reid, J. S., Maring, H. B., Narisma, G. T., van den Heever, S. C., DiGirolamo, L., Ferrare, R., et al. (2023). The coupling between tropical meteorology, aerosol science, convection and the energy budget during the Clouds, Aerosol Monsoon Processes Philippines Experiment (CAMP2Ex). *Bull. Amer. Met. Soc.*, *104*, E1179–E1209. https://doi.org/10.1175/BAMS-D-21-0285.1

Rotunno, R., Klemp, J. B., & Weisman, M. L. (1988). A theory for strong, long-lived squall lines. *Journal of the Atmospheric Sciences*, *45*(3), 463–485. https://doi.org/10.1175/1520-0469(1988)045<0463:ATFSLL>2.0.CO;2

Sakradzija, M. (2023). ICON-LES for FESSTVaL: Jogi cold pool 2021-06-29 (Version v1) [Dataset]. *Zenodo*. https://doi.org/10.5281/zenodo.8411098

Saleeby, S. M., & van den Heever, S. C. (2013). Developments in the CSU-RAMS aerosol model: Emissions, nucleation, regeneration, deposition, and radiation. *Journal of Applied Meteorology and Climatology*, *52*(12), 2601–2622. https://doi.org/10.1175/JAMC-D-12-0312.1

Schlemmer, L., & Hohenegger, C. (2014). The formation of wider and deeper clouds as a result of cold-pool dynamics. *Journal of the Atmospheric Sciences*, *71*(8), 2842–2858. https://doi.org/10.1175/JAS-D-13-0170.1

Seigel, R. B., & van den Heever, S. C. (2012). Dust lofting and ingestion by supercell storms. *Journal of the Atmospheric Sciences*, *69*(5), 1453–1473. https://doi.org/10.1175/JAS-D-11-0222.1

Simoes-Sousa, I. T., Tandon, A., Buckley, J., Sengupta, D., Sree, L. J., Shroyer, E., & de Szoeke, S. P. (2022). Atmospheric cold pools in the Bay of Bengal. *Journal of the Atmospheric Sciences*, *80*(1), 167–180. https://doi.org/10.1175/JAS-D-22-0041.1

Simpson, J. E. (1969). A comparison between laboratory and atmospheric density currents. *Q. J. Roy.Meteor. Soc.*, *95*(406), 758–765. https://doi.org/10.1002/qj.49709540609

Straka, J. M., Wilhelmson, R. B., Wicker, L. J., Anderson, J. R., & Droegemeier, K. K. (1993). Numerical solutions of a non-linear density current: A benchmark solution and comparisons. *International Journal for Numerical Methods in Fluids*, *17*(1), 1–22. https://doi.org/10.1002/fld.1650170103

Terai, C. R., & Wood, R. (2013). Aircraft observations of cold pools under marine stratocumulus. *Atmospheric Chemistry and Physics*, *13*(19), 9899–9914. https://doi.org/10.5194/ACP-13-9899-2013

van den Heever, S. C., Grant, L. D., Freeman, S. W., Marinescu, P. J., Barnum, J., Bukowski, J., et al. (2021). The Colorado state university convective CLoud outflows and UpDrafts experiment (C3LOUD-Ex). *Bulletin of the American Meteorological Society*, *102*(7), E1283–E1305. https://doi.org/10.1175/BAMS-D-19-0013.1

Wackernagel, H. (2003). *Multivariate geostatistics: An introduction with applications* (3rd ed.). Springer.

Wilson, J. W., & Schreiber, W. E. (1986). Initiation of convective storms at radar-observed boundary-layer convergence lines. *Monthly Weather Review*, *114*(12), 2516–2536. https://doi.org/10.1175/1520-0493(1986)114<2516:IOCSAR>2.0.CO;2

Zuidema, P., Li, Z., Hill, R. J., Bariteau, L., Rilling, B., Fairall, C., et al. (2012). On trade wind cumulus cold pools. *Journal of the Atmospheric Sciences*, *69*(1), 258–280. https://doi.org/10.1175/JAS-D-11-0143.1

References From the Supporting Information

Feranec, J., Soukup, T., Hazeu, G., & Jaffrain, G. (Eds.) (2016)., *European landscape dynamics. Corine land cover data* (pp. 9–14). CRC-Press.

Harrington, J. Y. (1997). *The effects of radiative and microphysical processes on simulated warm and transition season Arctic stratus*. Ph.D. dissertation (p. 301), Colorado State University.

Heinze, R., Dipankar, A., Henken, C. C., Moseley, C., Sourdeval, O., Trömel, S., et al. (2017). Large-eddy simulations over Germany using ICON: A comprehensive evaluation. *The Quarterly Journal of the Royal Meteorological Society*, *143*(702), 69–100. https://doi.org/10.1002/qj.2947

Hill, G. E. (1974). Factors controlling the size and spacing of cumulus clouds as revealed by numerical experiments. *Journal of the Atmospheric Sciences*, *31*(3), 646–673. https://doi.org/10.1175/1520-0469(1974)031<0646:FCTSAS>2.0.CO;2

19448007, 2024, 6, Downloaded from https://agupubs.onlinelibrary.wiley.com/doi/10.1029/2023GL106784, Wiley Online Library on [19/03/2024]. See the Terms and Conditions (https://onlinelibrary.wiley.com/terms-and-conditions) on Wiley Online Library for rules of use; OA articles are governed by the applicable Creative Commons License

Lilly, D. K. (1962). On the numerical simulation of buoyant convection. *Tellus*, *14*(2), 148–172. https://doi.org/10.1111/J.2153-3490.1962.TB00128.x

NASA/METI/AIST/Japan Spacesystems and U.S./Japan ASTER Science Team. (2019). *ASTER global digital elevation model V003*. NASA EOSDIS Land Processes Distributed Active Archive Center. https://doi.org/10.5067/ASTER/ASTGTM.003

Schulz, J.-P., & Vogel, G. (2020). Improving the processes in the land surface scheme TERRA: Bare soil evaporation and skin temperature. *Atmosphere*, *11*(5), 513. https://doi.org/10.3390/atmos11050513

Smagorinsky, J. (1963). General circulation experiments with the primitive equations. *Monthly Weather Review*, *91*(3), 99–164. https://doi.org/10.1175/1520-0493(1963)091<0099:GCEWTP>2.3.CO;2

Walko, R. L., Band, L. E., Baron, J., Kittel, T. G. F., Lammers, R., Lee, T. J., et al. (2000). Coupled atmosphere–biophysics–hydrology models for environmental modeling. *Journal of Applied Meteorology*, *39*(6), 931–944. https://doi.org/10.1175/1520-0450(2000)039<0931:CABHMF>2.0.CO;2

19448007, 2024, 6, Downloaded from https://agupubs.onlinelibrary.wiley.com/doi/10.1029/2023GL106784, Wiley Online Library on [19/03/2024]. See the Terms and Conditions (https://onlinelibrary.wiley.com/terms-and-conditions) on Wiley Online Library for rules of use; OA articles are governed by the applicable Creative Commons License